PHYSICAL REVIEW B **82**, 081104(R) (2010)

Broken symmetry, strong correlation, and splitting between longitudinal and transverse optical phonons of MnO and NiO from first principles

Yi Wang, James E. Saal, Jian-Jun Wang, Arkapol Saengdeejing, Shun-Li Shang, Long-Qing Chen, and Zi-Kui Liu
Materials Science and Engineering, The Pennsylvania State University, University Park, Pennsylvania 16802, USA
(Received 30 July 2010; published 18 August 2010)

We propose a first-principles scheme, using the distorted structure, to obtain the phonons of the undistorted parent structure for systems with both broken symmetry as well as the splitting between longitudinal optical and transverse optical (TO) phonon modes due to long-range dipole-dipole interactions. Broken symmetry may result from antiferromagnetic ordering or structural distortion. Applications to the calculations of the phonon dispersions of NiO and MnO, the two benchmark Mott-Hubbard systems with the TO mode splitting for MnO, show remarkable accuracy.

DOI: 10.1103/PhysRevB.82.081104 PACS number(s): 71.27.+a, 63.20.dk, 63.50.−x

With advances in calculating atomic force constants within the framework of density-functional perturbation theory[1] and density-functional theory,[2] first-principles calculations can now predict electronic and vibrational properties for many classes of materials, including simple metals, transition metals, intermetallics, semiconductors, hydrides, and earth materials with exceptional accuracy.[3] However, it has been difficult to predict the lattice dynamics for strongly correlated electronic systems, particularly Mott-Hubbard insulators. These include materials such as NiO and MnO,[4–8] the La_2CuO_4-based cuprate superconductors,[9] and the $LaMnO_3$-based colossal magnetoresistance manganites.[10] Experimental measurements also yielded inconsistent results on the frequency values of the optical phonons for both MnO (Refs. 6 and 8) and NiO.[5,7] The specific difficulties[11–15] in predicting the lattice dynamics of Mott-Hubbard insulators are: (i) the highly correlated nature of electronic states in these materials and (ii) the slight lowering of crystal symmetry as a result of antiferromagnetic ordering (~0.6° for MnO and ~0.07° for NiO away from cubic[16]).

In this work, we report a scheme to accurately compute phonon dispersions of Mott-Hubbard systems such as MnO and NiO. This involves a combination of a method for recovering the ideal cubic symmetry from the slightly distorted structure, the mixed-space approach[17] for treating the splitting between longitudinal optical (LO) and transverse optical (TO) phonon modes, and the density-functional theory (DFT) plus U method for accounting for the strong electron correlation.[18]

In applying the direct approach to predict the phonon dispersions of polar materials, a lot of effort[19–23] has been made to treat the contribution of the nonanalytical term. The mixed-space approach makes it parameter-free to accurately determine the phonon frequencies using the direct approach for polar materials.[17] In this approach, the force constants are written as

$$\Phi_{\alpha\beta}^{jk}(M,P) = \phi_{\alpha\beta}^{jk}(M,P) + \frac{1}{N}\tilde{D}_{\alpha\beta}^{jk}(na;\mathbf{q}\to 0), \tag{1}$$

where $\Phi_{\alpha\beta}^{jk}$ is the interaction force-constant between atom j in the primitive cell M and atom k in the primitive cell P, $\phi_{\alpha\beta}^{jk}$ the contribution from short-range interactions, N the number of primitive unit cells in the supercell, and $\tilde{D}_{\alpha\beta}^{jk}(na;\mathbf{q}\to 0)$ the contribution from long-range interactions, i.e., the so-called nonanalytical part of the dynamical matrix in the limit of zero wave vector $\mathbf{q}$. According to Cochran and Cowley[24]

$$\tilde{D}_{\alpha\beta}^{jk}(na;\mathbf{q}\to 0) = \frac{4\pi e^2}{V}\left.\frac{[\mathbf{q}\cdot\mathbf{Z}^*(j)]_\alpha[\mathbf{q}\cdot\mathbf{Z}^*(k)]_\beta}{\mathbf{q}\cdot\boldsymbol{\varepsilon}_\infty\cdot\mathbf{q}}\right|_{\mathbf{q}\to 0}, \tag{2}$$

where V is the volume of the primitive unit cell, $\mathbf{q}$ the wave vector, α and β the Cartesian axes, $\mathbf{Z}^*(j)$ the Born effective charge tensor of the jth atom in the primitive unit cell, and $\boldsymbol{\varepsilon}_\infty$ the high-frequency static dielectric tensor, i.e., the contribution to the dielectric permittivity tensor from the electronic polarization.[1] As a result, the dynamical matrix $\tilde{D}_{\alpha\beta}^{jk}(\mathbf{q})$ can be calculated by the following Fourier transformation:[25]

$$\begin{aligned}\tilde{D}_{\alpha\beta}^{jk}(\mathbf{q}) &= \frac{1}{\sqrt{\mu_j\mu_k}}\frac{1}{N}\sum_{M,P}\Phi_{\alpha\beta}^{jk}(M,P)\exp\{i\mathbf{q}\cdot[\mathbf{R}(P)-\mathbf{R}(M)]\}\\ &= \frac{1}{\sqrt{\mu_j\mu_k}}\frac{1}{N}\sum_{M,P}\phi_{\alpha\beta}^{jk}(M,P)\exp\{i\mathbf{q}\cdot[\mathbf{R}(P)-\mathbf{R}(M)]\}\\ &\quad+\tilde{D}_{\alpha\beta}^{jk}(na;\mathbf{q}),\end{aligned} \tag{3}$$

where μ_j is the atomic mass of the jth atom in the primitive unit cell, $\mathbf{R}(P)$ the position of the Pth primitive unit cell in the supercell, and $\tilde{D}_{\alpha\beta}^{jk}(na;\mathbf{q})$ the so-called nonanalytical contribution to the dynamical matrix.

$$\begin{aligned}\tilde{D}_{\alpha\beta}^{jk}(na,\mathbf{q}) &= \tilde{D}_{\alpha\beta}^{jk}(na,\mathbf{q}\to 0)\frac{1}{\sqrt{\mu_j\mu_k}}\frac{1}{N^2}\sum_{M,P}\\ &\quad\times\exp\{i\mathbf{q}\cdot[\mathbf{R}(P)-\mathbf{R}(M)]\}.\end{aligned} \tag{4}$$

Equation (3) was originally derived to consider surface effects.[25] For the present purpose, the summation over M serves as a dynamic average over the symmetry breaking due to magnetic ordering or lattice distortion.

For first-principles static calculations at 0 K, we employed the projector-augmented-wave method[26,27] together with the Dudarev DFT+U method[18] implemented in the Vienna *ab initio* simulation package (VASP, version 5.2). We have followed the suggestions by Anisimov *et al.*[13] and by Savrasov and Kotliar[14] to use large U values. The calculated

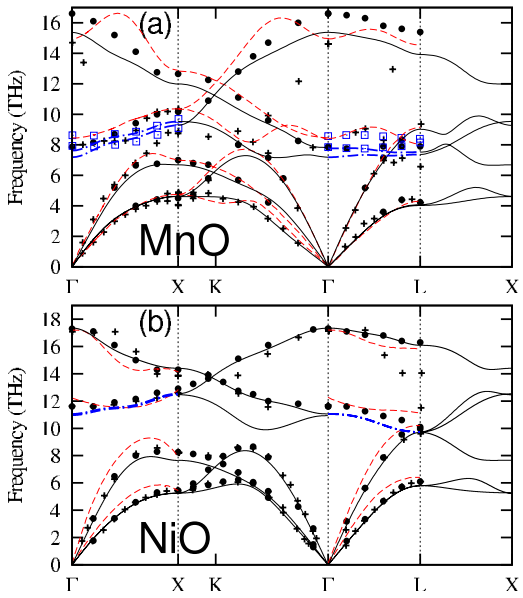

FIG. 1. (Color online) Phonon dispersions of the rhombohedral MnO and NiO, expressed using the symmetry of the cubic structure. The calculated phonon dispersions by this work with TO splitting along the Γ-X and Γ-L directions due to symmetry breaking are represented by the dot-dashed (blue) curves, and the calculated phonon dispersions by this work without splitting are represented by solid (black) curves. (a) MnO: the crosses, the filled circles, and the open (blue) squares represent the measured data by Haywood and Collins (Ref. 6), Wagner *et al.* (Ref. 8), and Chung *et al.* (Ref. 4), respectively; the dashed (red) curves are from the calculations by Wdowik and Legut (Ref. 15); and (b) NiO: the crosses and the circles represent the measured data by Coy *et al.* (Ref. 15) and Reichardt *et al.* (Ref. 7), respectively; the dashed (red) curves are from the DMFT calculations by Savrasov and Kotliar. (Ref. 14)

results of Dudarev DFT+U approach only depend on the difference of U-J, and we assigned U-J=7.55 eV for the d orbital of Ni and U-J=6.9 eV for the d orbital of Mn according to Wdowik and Legut.[15] The exchange-correlation functional of generalized gradient approximation (GGA) according to Perdew-Burke-Ernzerhof (Ref. 28) was employed in all calculations. To find the theoretical equilibrium static geometries for MnO and NiO, we used a Γ-centered $15\times15\times15$ k mesh together with an energy cutoff of 500 eV. To calculate the Born effective charge tensor, we employed the linear-response theory implemented in VASP 5.2 by Gajdoš *et al.*[29] In calculating the real-space force constants, we used 128 atom $4\times4\times4$ supercells and a Γ-centered $3\times3\times3$ k mesh.

In Fig. 1, we show the calculated phonon frequencies for MnO and NiO at their theoretical equilibrium geometries together with the measured data.[4–8] Note that for both MnO (Refs. 6 and 8) and NiO (Refs. 5 and 7) different experimental investigations find different behavior in the optical branches of the phonon dispersions. Wagner *et al.*[8] pointed out that their room-temperature phonon dispersions for MnO measured for a flame-grown single crystal of 4 cm^3 using a three-axis crystal spectrometer were more reliable than the measurement by Haywood and Collins[6] who used a small pillar about 5 mm^2 by 2 cm and a beryllium filter technique, which inherently has low q-space resolution. For NiO, both measurements by Reichardt *et al.*[7] and Coy *et al.*[5] were performed using three-axis crystal spectrometers at room temperature. However, the measured data by Reichardt *et al.* have been more widely cited than those by Coy *et al.* Our calculated results strongly support the frequently cited experiments for NiO by Reichardt *et al.*[7] and for MnO by Wagner *et al.*[8]

The calculated phonon dispersions of MnO by Wdowik and Legut[15] and the calculated phonon dispersions of NiO by Savrasov and Kotliar[14] are also plotted in Fig. 1. Substantial overall improvement in the present calculations can be seen over these two previous theoretical calculations. Although Wdowik and Legut found the best U-J value for Mn in MnO, large errors still exist in their calculated phonon frequencies for the optical branches, perhaps due to: (i) the 64-atom supercell and $2\times2\times2$ k mesh were not large enough and (ii) the semiempirical extrapolation by Parlinski *et al.*[30] was not suitable for describing the LO-TO splitting. It seems that Wdowik and Legut did not consider the experiment by Wagner.[8] In a Letter, Savrasov and Kotliar[14] calculated the phonon frequencies of MnO and NiO by introducing a linear-response method within the framework of the local-density approximation (LDA) and the dynamical mean-field theory (DMFT). It appears that Savrasov and Kotliar[14] only compared their calculations with the experiments by Coy *et al.*[5] and Haywood *et al.*[6] and did not consider the experiments for NiO by Reichardt *et al.*[7] and for MnO by Wagner.[8] The DMFT calculations by Savrasov and Kotliar adopted the paramagnetic state for NiO, which might not be suitable to describe the room-temperature properties of NiO since the experimental Néel temperature (T_N) of NiO is 523 K,[7] and may be a reason the current calculations see such large improvements.

By using the local spin-density approximation with model corrections, Massidda *et al.*[31] predicted that the low-frequency zone-center optic modes of MnO should exhibit an anisotropic splitting as large as 10% of their energy due to the anisotropy of the electronic response as a consequence of magnetic ordering. We indeed observe small phonon frequency splitting of the TO modes along the (ξ00) and ($\xi\xi\xi$) directions in our calculated results for MnO, in quantitative agreement with an experiment by Chung *et al.*[4] which showed such a splitting. Furthermore, the present calculations show that the splitting is direction dependent in the **q** space. This splitting was also qualitatively predicted by the frozen phonon calculations at the Γ point of Luo *et al.*[32] However, our calculations for NiO show an almost invisible TO splitting, in disagreement with the measurement of Chung *et al.*[4] The frozen phonon calculations of Luo *et al.*[32] even showed an opposite sign of the splitting for NiO. Chung *et al.*[4] stated in their paper that their NiO crystal was of less reliable quality than their MnO crystal. Luo *et al.*[32] pointed out, by their private communication with Chung *et al.* (Ref. 12 of Luo *et al.*[32]) that the published results of Chung *et al.*[4] for NiO were much less conclusive than those for MnO due to the experimental difficulties that were specific to NiO. In comparison, the DMFT calculations[14] did not show the TO splitting due to the use of the paramagnetic state.

As a consequence of magnetic ordering, both the crystal

TABLE I. Calculated lattice constants a(Å), rhombohedral distortion angles θ(°), Born effective charges $|Z^*|(e)$, high-frequency static dielectric constants ε_∞, LO phonon frequency ω_{LO}(THz), TO phonon frequencies ω_{TO1} and ω_{TO2}(THz), and splitting between the two TO phonon frequency $\Delta\omega_{TO}$(THz) of NiO and MnO, in comparison with those of the previous DMFT calculations (Ref. 14) and experiments (Refs. 4–8, 16, 33, and 34).

	a	θ	$\lvert Z^*\rvert$	ε_∞	ω_{LO}	ω_{TO1}	ω_{TO2}	$\Delta\omega_{TO}$
				MnO				
DFT+U [a]	4.5061	90.504	2.27	4.42	15.37	7.19	7.62	0.43
DMFT[b]			2.3	5.7	15.3	8.9	8.9	0
Expt.	4.4315[c]	90.60[c]	2.2[d]	5.0[e]	14.51[f]	7.86[f]	7.86[f]	
					16.6[g]	7.86[g]	7.86[g]	
						8.05[h]	8.80[h]	0.75[h]
				NiO				
DFT+U [a]	4.1929	90.045	2.10	4.66	17.35	10.97	11.05	0.08
DMFT[b]			2.3	6.9	17.1	12.2	12.2	0
Expt.	4.1704[c]	90.08[c]	2.2[d]	5.7[i]	17.07[j]	11.63[j]	11.63[j]	
					17.3[k]	11.6[k]	11.6[k]	

[a]Antiferromagnetic calculations of the present work.
[b]Paramagnetic calculations by Savrasov and Kotliar (Ref. 14).
[c]Cheetham (Ref. 16).
[d]Estimated from ω_{LO}, ω_{TO}, and ε_∞ in Ref. 14.
[e]Plendl *et al.* (Ref. 34).
[f]At room temperature, Haywood and Collins (Ref. 6).
[g]At 296 K, Wagner *et al.* (Ref. 8).
[h]At 4.3 K, Chung *et al.* (Ref. 4).
[i]Gielisse *et al.* (Ref. 33).
[j]At room temperature, Coy *et al.* (Ref. 5).
[k]At room temperature, Reichardt *et al.* (Ref. 7).

distortion and the splitting of the TO modes are seen, depending on the anisotropy of the electronic response. The very small TO splitting in NiO predicted by the present calculation implies that the anisotropy of the electronic response is weaker in NiO than in MnO. This agrees with the experimental observation that the measured distortion away from ideal cubic for NiO is just ~0.07° which is almost one magnitude smaller than that of ~0.6° for MnO.

Table I summarizes the calculated lattice constants a(Å), the rhombohedral distortion angles θ, Born effective charges Z^*, the high-frequency static dielectric constants ε_∞, the LO phonon frequency ω_{LO}, the TO phonon frequencies ω_{TO1} and ω_{TO2}, and the splitting between the two TO phonon frequency $\Delta\omega_{TO}$ of NiO and MnO, in comparison with those of the previous DMFT calculations by Savrasov and Kotliar[14] and experiments.[4–8,16,33,34] We note that the experimental Z^*'s listed in Table I are estimated values from ω_{LO}, ω_{TO}, and ε_∞ by Savrasov and Kotliar.[14] The calculated lattice parameters are 1.7% and 0.5% larger than those from experiment,[16] respectively. These overestimations are quite normal when the GGA exchange-correlation functional is applied to oxides. For Z^* and ε_∞, the present calculations lead to values smaller than those of DMFT and experiments.[33,34] The present work has underestimated the high-frequency dielectric constant values in comparison to experiments since we have used larger U-J values. The differences between the present calculations and those of DMFT could be due in part to the fact that our values are from GGA+U at theoretical 0 K geometries and those of DMFT are from LDA+DMFT (Ref. 14) at the experimental geometries. Very detailed discussions of the effects of U-J values on Z^*, ε_∞, and phonon frequencies for MnO have been discussed by Wdowik and Legut[15] who found that large U-J values enhance the on-site force constant for Mn, localize more strongly the 3d electrons of Mn, and prevent charge flow. In our work, we attempt to have all physical quantities calculated by the first-principles method. The purpose of the present work is to calculate the phonon frequencies and employ Z^* and ε_∞ to predict the LO-TO splitting. We believe that the Z^* and ε_∞ values differences among the present calculations, DMFT,

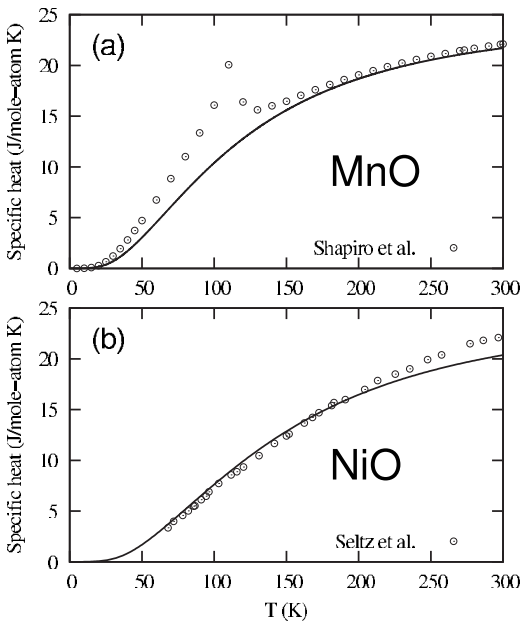

FIG. 2. Calculated specific heats (solid curves) of (a) MnO and (b) NiO in comparison with the experimental data (open circles) for MnO by Shapiro *et al.* (Ref, 36) and NiO by Seltz *et al.* (Ref. 35).

and experiments change the basic physical features of the present work.

We have also calculated the constant volume heat capacities of MnO and NiO at temperature ranges up to 300 K for the rhombohedral structure, and results are compared in Fig. 2 with the measured zero pressure values.[35,36] For MnO, the experimental peak below 150 K is due to the magnetic Néel phase transition[36] (T_N=118 K) which is not considered in the present work. The deviation between the present theory and the measurement for NiO above 200 K is also due to neglecting the magnetic contribution in the present work [the experimental T_N of NiO is 523 K (Ref. 7)].

In summary, we resolved the long-standing issue of discrepancies between theory and experiment in lattice dynamics of MnO and NiO by implementing a first-principles scheme to predict the phonon frequencies of systems with both broken symmetry due to magnetic ordering and slight structural distortion. Excellent agreement with experiments for the overall phonon dispersions are obtained for both MnO and NiO, particularly the phonon splitting of the TO mode for MnO. The accomplishment of the present work goes far beyond the specific systems of MnO and NiO. For example, the same scheme can be applied to understand the phonon properties of La_2CuO_4-based superconductors[9] and $LaMnO_3$-based colossal magnetoresistance manganites.[10]

This work was funded by the Office of Naval Research (ONR) under Contract No. N0014-07-1-0638, the National Science Foundation (NSF) under Grant No. DMR-1006557, DOE Basic Sciences under Grant No. DOE DE-FG02-07ER46417 (Yi Wang and Chen), and in part supported by instrumentation funded by the National Science Foundation under Grant No. OCI-0821527. Calculations were also conducted at the LION clusters at the Pennsylvania State University and at the National Energy Research Scientific Computing Center, which is supported by the Office of Science of the U.S. Department of Energy under Contract No. DE-AC02-05CH11231. This work was also supported in part by a grant of HPC resources from the Arctic Region Supercomputing Center at the University of Alaska Fairbanks as part of the Department of Defense High Performance Computing Modernization Program.

[1] S. Baroni, S. de Gironcoli, A. Dal Corso, and P. Giannozzi, Rev. Mod. Phys. **73**, 515 (2001).
[2] A. van de Walle and G. Ceder, Rev. Mod. Phys. **74**, 11 (2002).
[3] S. Baroni, P. Giannozzi, and E. Isaev, Rev. Mineral. Geochem. **71**, 39 (2010).
[4] E. M. L. Chung, D. M. Paul, G. Balakrishnan, M. R. Lees, A. Ivanov, and M. Yethiraj, Phys. Rev. B **68**, 140406 (2003).
[5] R. A. Coy, C. W. Tompson, and E. Gurmen, Solid State Commun. **18**, 845 (1976).
[6] B. C. Haywood and M. F. Collins, J. Phys. C **4**, 1299 (1971).
[7] W. Reichardt, V. Wagner, and W. Kress, J. Phys. C **8**, 3955 (1975).
[8] V. Wagner, W. Rechhardt, and W. Kress, in *Proceedings of the Conference on Neutron Scattering*, edited by R. M. Moon (NTIS, Springfield, VA, Gatlinburg, 1976), Vol. 1, p. 175.
[9] J. G. Bednorz and K. A. Muller, Z. Phys. B: Condens. Matter **64**, 189 (1986).
[10] J. Fontcuberta, B. Martinez, A. Seffar, S. Pinol, J. L. Garcia-Munoz, and X. Obradors, Phys. Rev. Lett. **76**, 1122 (1996).
[11] V. I. Anisimov, F. Aryasetiawan, and A. I. Lichtenstein, J. Phys.: Condens. Matter **9**, 767 (1997).
[12] V. I. Anisimov, M. A. Korotin, and E. Z. Kurmaev, J. Phys.: Condens. Matter **2**, 3973 (1990).
[13] V. I. Anisimov, J. Zaanen, and O. K. Andersen, Phys. Rev. B **44**, 943 (1991).
[14] S. Y. Savrasov and G. Kotliar, Phys. Rev. Lett. **90**, 056401 (2003).
[15] U. D. Wdowik and D. Legut, J. Phys.: Condens. Matter **21**, 275402 (2009).
[16] A. K. Cheetham and D. A. O. Hope, Phys. Rev. B **27**, 6964 (1983).
[17] Y. Wang, J. J. Wang, W. Y. Wang, Z. G. Mei, S. L. Shang, L. Q. Chen, and Z. K. Liu, J. Phys.: Condens. Matter **22**, 202201 (2010).
[18] S. L. Dudarev, L. M. Peng, S. Y. Savrasov, and J. M. Zuo, Phys. Rev. B **61**, 2506 (2000).
[19] P. Giannozzi, S. Degironcoli, P. Pavone, and S. Baroni, Phys. Rev. B **43**, 7231 (1991).
[20] X. Gonze, J. C. Charlier, D. C. Allan, and M. P. Teter, Phys. Rev. B **50**, 13035 (1994).
[21] X. Gonze and C. Lee, Phys. Rev. B **55**, 10355 (1997).
[22] G. Kern, G. Kresse, and J. Hafner, Phys. Rev. B **59**, 8551 (1999).
[23] K. Kunc and R. M. Martin, Phys. Rev. Lett. **48**, 406 (1982).
[24] W. Cochran and R. A. Cowley, J. Phys. Chem. Solids **23**, 447 (1962).
[25] D. C. Wallace, *Thermodynamics of Crystals* (Wiley, New York, London, Sydney, Toronto, 1972).
[26] P. E. Blöchl, Phys. Rev. B **50**, 17953 (1994).
[27] G. Kresse and D. Joubert, Phys. Rev. B **59**, 1758 (1999).
[28] J. P. Perdew, K. Burke, and M. Ernzerhof, Phys. Rev. Lett. **77**, 3865 (1996).
[29] M. Gajdoš, K. Hummer, G. Kresse, J. Furthmüller, and F. Bechstedt, Phys. Rev. B **73**, 045112 (2006).
[30] K. Parlinski, Z. Q. Li, and Y. Kawazoe, Phys. Rev. Lett. **81**, 3298 (1998).
[31] S. Massidda, M. Posternak, A. Baldereschi, and R. Resta, Phys. Rev. Lett. **82**, 430 (1999).
[32] X. H. Luo, W. Zhou, S. V. Ushakov, A. Navrotsky, and A. A. Demkov, Phys. Rev. B **80**, 134119 (2009).
[33] P. J. Gielisse, J. N. Plendl, L. C. Mansur, R. Marshall, S. S. Mitra, R. Mykolajewycz, and A. Smakula, J. Appl. Phys. **36**, 2446 (1965).
[34] J. N. Plendl, L. C. Mansur, S. S. Mitra, and I. F. Chang, Solid State Commun. **7**, 109 (1969).
[35] H. Seltz, B. J. DeWitt, and H. J. McDonald, J. Am. Chem. Soc. **62**, 88 (1940).
[36] J. L. Shapiro, B. F. Woodfield, R. Stevens, and J. Boerio-Goates, J. Chem. Thermodyn. **31**, 725 (1999).